Available online at www.sciencedirect.com
SCIENCE DIRECT®
Journal of Solid State Chemistry 179 (2006) 685–695
JOURNAL OF SOLID STATE CHEMISTRY
www.elsevier.com/locate/jssc

Crystal structure, vibrational properties and luminescence of $NaMg_3Al(MoO_4)_5$ crystal doped with Cr^{3+} ions

K. Hermanowicz[a], M. Mączka[a,*], M. Wołcyrz[a], P.E. Tomaszewski[a], M. Paściak[a], J. Hanuza[a,b]

[a]*Institute of Low Temperature and Structure Research, Polish Academy of Sciences, P.O. Box 1410, 50-950 Wrocław 2, Poland*
[b]*Department of Bioorganic Chemistry, Faculty of Industry and Economics, University of Economics, ul. Komandorska 118/120, 53-345 Wrocław, Poland*

Received 6 September 2005; received in revised form 8 November 2005; accepted 18 November 2005
Available online 4 January 2006

Abstract

Crystals of $NaMg_3Al(MoO_4)_5$ doped with 0.5% Cr^{3+} ions have been synthesized and characterized by a single-crystal X-ray structure analysis and IR, Raman, electron absorption and luminescence spectroscopic studies. It has been shown that $NaMg_3Al(MoO_4)_5$ crystallizes in the $P\bar{1}$ structure, with $a = 6.8744(8)$ Å, $b = 6.9342(7)$ Å, $c = 17.605(2)$ Å, $\alpha = 87.788(8)^\circ$, $\beta = 87.727(9)^\circ$, $\gamma = 78.501(9)^\circ$, $Z = 2$. The characteristic feature of the structure is its enormously large thermal displacement parameter for sodium, even at 105 K. The IR and Raman spectra indicate significant interactions between the MoO_4^{2-} ions in the structure. The electron absorption, excitation and luminescence studies have shown that there are at least two different sites of incorporated Cr^{3+} ions in the $NaMg_3Al(MoO_4)_5$ crystal structure. They differ themselves by strength of crystalline field. One of them is characterized by Cr^{3+} in low ligand field and $^4T_2 \rightarrow {}^4A_2$ emission whereas the second is characterized by higher strength of the crystal field and dominant $^2E \rightarrow {}^4A_2$ emission. Temperature-dependent studies show that the compound does not exhibit any phase transition.

Keywords: Phonon properties; Electronic transitions; Crystal structure; Molybdates

1. Introduction

Molybdates have found many applications, for example as catalysts, laser materials, solid-state electrolytes [1–5]. Recently, a new group of ternary molybdates with general formula $NaM^{II}_3M^{III}(MoO_4)_5$, where M^{II} = Mg, Ni, Co, Mn, Fe; M^{III} = Al, In, Fe, Cr; has drawn attention since these molybdates may find application as solid-state electrolytes with sodium cation conductivity [6–8]. The iron containing molybdates are also suitable model systems for magnetic interactions because in this structure FeO_6 octahedra are separated from each other by MoO_4 tetrahedra and sodium ions [9]. These molybdates may also find application as catalysts in oxidation reactions since both magnesium, iron, nickel, cobalt and chromium molybdates are well-known catalysts [10–13].

The synthesis of the title $NaMg_3Al(MoO_4)_5$ crystals was described for the first time in Ref. [14]. It was shown that the crystals grow at high temperature and crystallize in triclinic system. Lattice parameters of $NaMg_3Al(MoO_4)_5$ were determined from powder diffraction data and schematic structure was suggested. However, the crystal structure was not solved and the atomic coordinates were not given. Later on, the isomorphous structure of $NaMg_3In(MoO_4)_5$ was solved [15]. Its triclinic unit cell dimensions are: $a = 7.0476(7)$ Å, $b = 17.935(2)$ Å, $c = 6.9849(7)$ Å, $\alpha = 87.650(9)^\circ$, $\beta = 100.980(8)^\circ$, $\gamma = 92.510(9)^\circ$; $Z = 2$ and space group $P\bar{1}$. The framework of this structure is similar to that observed for the $M^{III}_2(MoO_4)_3$ type of compounds (M^{III} = Fe, In, Sc, Al), which are well known to exhibit many important properties

*Corresponding author. Fax: +48 71 344 1029.
E-mail address: m.maczka@int.pan.wroc.pl (M. Mączka).

0022-4596/$ - see front matter © 2005 Elsevier Inc. All rights reserved.
doi:10.1016/j.jssc.2005.11.032

due to flexibility of the structure: high-ionic conductivity of trivalent ions, amorphization at low pressures, negative thermal expansion and ferroelastic phase transitions [16–20]. However, in the case of ternary molybdate some large cavities formed by MoO_4 tetrahedra and $(Mg,In)O_6$ octahedra, which are empty in the $M_2^{III}(MoO_4)_3$ structure, are occupied by Na^+ ions. It was also shown that Mg and In atoms occupy common positions with occupation 0.75 Mg + 0.25 In and that the sodium atom has an extremely large thermal displacement parameter which inclined the authors to split its positions into two, placed in a very short distance of 0.618 Å one from another.

Another isomorphous structure, $NaFe_4(MoO_4)_5$, was solved recently [9] as one of four new structures within Na–Fe–Mo–O system. Its lattice parameters are the following: $a = 6.9337(3)$ Å, $b = 7.0196(4)$ Å, $c = 17.8033(8)$ Å, $\alpha = 87.468(4)^\circ$, $\beta = 87.615(4)^\circ$, $\gamma = 79.090(4)^\circ$; $Z = 2$ and space group $P\bar{1}$. Also here, thermal displacement parameter for sodium is enormously large and anisotropic. Moreover, anomalous thermal displacement parameters of Na atoms were observed in many molybdates, e.g. $NaIn(MoO_4)_2$ [21], $Na_5Sc(MoO_4)_4$ [22], $Na_2Zr(MoO_4)_3$ [23], $Na_2Mg_5(MoO_4)_6$ [24] but without more detailed analysis of this phenomenon.

In the present paper we report on temperature-dependent X-ray diffraction, Raman, IR, luminescence and electron absorption studies of $NaMg_3Al(MoO_4)_5$ crystal, which belongs to this family of ternary molybdates, in order to get information about structure at different temperatures, in particular the behavior of sodium in the crystal structure and possible phase transitions. Our aim was also to characterize the vibrational properties of this material since such information is necessary to explain luminescence properties. We would like to emphasize that vibrational properties of this family of ternary molybdates have not yet been studied.

$NaMg_3Al(MoO_4)_5$ compound was chosen for these studies for a few reasons. Firstly, the structure of this material has not yet been reported. Secondly, whereas in the previously studied $NaMg_3In(MoO_4)_5$ the Mg^{2+} and In^{3+} ions are disordered among the same crystallographic positions due to similarity of ionic radii, we expected to observe ordering of Al^{3+} and Mg^{2+} ions due to significantly different ionic radii of these ions. Thirdly, we expected to observe more efficient luminescence of Cr^{3+} ions doped in this material, when compared with the indium analog, due to the small ionic size of Al^{3+} ions and, consequently, stronger crystal field.

2. Experiment

Single crystals of $NaMg_3Al(MoO_4)_5$: 0.5% Cr^{3+} were grown by cooling of the molten mixture containing MgO (99.99%), Na_2CO_3 (99.5%), Al_2O_3 (99.99%), Cr_2O_3 (99.995%) and MoO_3 (99.95%). The amount of chemicals used corresponded to composition $NaMg_3Al(MoO_4)_5$: 0.5% Cr^{3+} and $Na_2Mo_2O_7$ in a ratio of 1:2. The mixture was kept at 950 °C for 20 h, cooled with a 2 °C/h rate to 600 °C and 10 °C/h rate down to room temperature (RT). The obtained good quality, not twinned crystals were separated from the $Na_2Mo_2O_7$ solvent by washing with hot water. Dimensions of the crystals were up to $3 \times 2 \times 2$ mm.

Single crystal of $NaMg_3Al(MoO_4)_5$ was measured twice, at RT (293 K) and at 105 K, on Oxford Diffraction X'Calibur four-circle single-crystal diffractometer equipped with CCD detector using graphite-monochromatized Mo$K\alpha$ radiation ($\lambda = 0.71073$ Å). Oxford Cryosystem liquid nitrogen attachment was applied to the measurement at 105 K. The intensities of the reflections were corrected for Lorentz and polarization factors. Analytical absorption correction was applied.

The crystal structure was solved by Patterson methods and refined by full matrix least-squares method using SHELX-97 program [25]. Refinement was performed on F^2 against all reflections. The weighted R factor (wR) and goodness of fit (S) are based on F^2, conventional R factors (R) are based on F, with F set to zero for negative

Table 1
Crystal data and structure refinement for $NaMg_3Al(MoO_4)_5$

Empirical formula	$NaMg_3Al(MoO_4)_5$	
Formula weight	922.60	
Z	2	
Crystal system, space group	Triclinic, $P\bar{1}$ (No. 2)	
Temperature	105 (0.5) K	293(1) K
Unit cell dimensions	$a = 6.8742(8)$ Å	$a = 6.8744(8)$ Å
	$b = 6.9305(7)$ Å	$b = 6.9342(7)$ Å
	$c = 17.575(2)$ Å	$c = 17.605(2)$ Å
	$\alpha = 87.902(8)^\circ$	$\alpha = 87.788(8)^\circ$
	$\beta = 87.648(9)^\circ$	$\beta = 87.727(9)^\circ$
	$\gamma = 78.942(15)^\circ$	$\gamma = 78.501(9)^\circ$
Volume	820.73(15) Å^3	821.28(15) Å^3
Calculated density	3.733 mg/m^3	3.731 mg/m^3
Absorption coefficient	4.018 mm^{-1}	4.016 mm^{-1}
$F(000)$	860	860
Crystal size	$0.375 \times 0.175 \times 0.008$ mm	$0.375 \times 0.175 \times 0.008$ mm
θ range for data collection	4.38–33.10°	3.20–33.00°
Limiting indices	$-10 \leqslant h \leqslant 10$	$-10 \leqslant h \leqslant 10$
	$-10 \leqslant k \leqslant 10$	$-10 \leqslant k \leqslant 10$
	$0 \leqslant l \leqslant 26$	$0 \leqslant l \leqslant 26$
Reflections collected/ unique	10978	11369
Independent reflections	5209	5207
R_{int}	0.0343	0.0355
Completeness to $\theta = 25.25$	99.6%	99.4%
Data/parameters	5209/272	5207/272
Goodness-of-fit on F^2	1.568	1.465
Final R indices $[I > 2\sigma(I)]$	$R_1 = 0.0292$, w$R_2 = 0.0749$	$R_1 = 0.0255$, w$R_2 = 0.0703$
R indices (all data)	$R_1 = 0.0303$, w$R_2 = 0.0753$	$R_1 = 0.0262$, w$R_2 = 0.0706$
Extinction coefficient	0.0039(3)	0.0040(2)
Largest diff. peak and hole	3.320 and −1.868 e/Å^{-3}	2.287 and −1.708 e/Å^{-3}

experimental F^2. For both refinements anisotropic thermal displacement parameters were applied. According to very similar atomic numbers of Mg and Al it was not possible to settle a question of mixing of these atoms as, e.g. in [15]. The refinement with different mixing schema gave the same results. Therefore, the structure was refined as consisting of fully ordered Mg and Al sites. 0.5% doping of Cr^{+3} ions was not taken into account during the refinement procedure. The crystal data and the essential structure refinement details for both temperatures studied are given in Table 1.

Polycrystalline infrared spectra were measured with a Biorad 575C FT-IR spectrometer as KBr pellets in the 1500–400 cm^{-1} region and in Nujol suspension for the 500–30 cm^{-1} region. Raman spectra were recorded in 180° scattering geometry with a Bruker FT-Raman RFS 100/S spectrometer. 1064 nm line of a YAG:Nd^{3+} laser was used as an excitation source. Blackman–Harris four-term apodization was applied and the number of collected scans was 64. Temperature-dependent studies of IR and Raman spectra were performed using a helium-flow cryostat (Oxford Instruments, CF 1204). The IR and Raman spectra were recorded with a spectral resolution of 2 cm^{-1}.

The absorption spectra were recorded using Cary 5E spectrophotometer with the 0.02 nm resolution. The focal length of the monochromator was 25 cm. The grating has 1200 lines/mm.

The emission and excitation spectra were recorded on a SSF-01 spectrofluorimeter with gratings of 1200 lines/mm. As excitation source a 150 mW xenon lamp was used. The excitation line was 491 nm.

Table 2
Atomic coordinates ($\times 10^4$) and equivalent isotropic displacement parameters ($Å^2 \times 10^3$) for $NaMg_3Al(MoO_4)_5$

Atom	105 K				293 K			
	x	y	z	U_{eq}	x	y	z	U_{eq}
Mo1	2726(1)	604(1)	9043(1)	5(1)	2730(1)	605(1)	9041(1)	8(1)
Mo2	−2150(1)	1755(1)	7154(1)	6(1)	−2157(1)	1761(1)	7154(1)	9(1)
Mo3	−7300(1)	3087(1)	5278(1)	6(1)	−7307(1)	3090(1)	5281(1)	9(1)
Mo4	−2466(1)	4537(1)	9140(1)	7(1)	−2464(1)	4536(1)	9143(1)	10(1)
Mo5	−6799(1)	−2202(1)	6918(1)	8(1)	−6802(1)	−2189(1)	6917(1)	11(1)
Mg1	−1841(2)	1710(2)	5070(1)	5(1)	−1849(1)	1708(1)	5076(1)	7(1)
Mg2	−7790(2)	5747(2)	8735(1)	4(1)	−7786(1)	5748(1)	8734(1)	7(1)
Mg3	−1678(2)	9168(2)	8845(1)	5(1)	−1680(1)	9172(2)	8849(1)	8(1)
Al	−7516(2)	3044(2)	7358(1)	8(1)	−7525(1)	3053(1)	7355(1)	11(1)
Na	−1099(3)	−3350(3)	6896(2)	46(1)[a]	−1117(3)	−3343(3)	6902(2)	80(1)[a]
O1	1443(4)	−1297(3)	8811(1)	8(1)	1449(3)	−1296(3)	8811(1)	11(1)
O2	−4814(4)	2104(4)	5064(2)	13(1)	−4821(4)	2104(4)	5077(2)	21(1)
O3	−7560(4)	3510(4)	6260(2)	16(1)	−7593(4)	3514(4)	6258(2)	22(1)
O4	−8191(4)	−1997(4)	6093(2)	13(1)	−8165(4)	−1988(4)	6089(2)	19(1)
O5	−1925(4)	1208(4)	6198(2)	12(1)	−1905(4)	1202(4)	6200(2)	19(1)
O6	−4801(4)	5399(4)	8763(2)	13(1)	−4801(4)	5390(4)	8767(2)	21(1)
O7	−2489(4)	4669(4)	10126(2)	14(1)	−2495(4)	4662(4)	10128(2)	21(1)
O8	−8771(4)	1326(4)	5032(1)	10(1)	−8771(3)	1337(3)	5026(1)	14(1)
O9	−7999(4)	5347(4)	4782(2)	12(1)	−7991(4)	5343(4)	4782(2)	18(1)
O10	−4618(4)	2865(4)	7366(2)	13(1)	−4631(4)	2862(4)	7355(2)	20(1)
O11	−490(4)	3377(4)	7330(1)	11(1)	−509(4)	3390(4)	7333(1)	17(1)
O12	−7746(4)	−4010(4)	7542(2)	11(1)	−7748(3)	−4003(3)	7540(1)	14(1)
O13	−7127(4)	139(4)	7330(2)	15(1)	−7150(4)	149(4)	7324(2)	23(1)
O14	2317(4)	2889(4)	8483(1)	9(1)	2321(3)	2893(3)	8480(1)	12(1)
O15	2055(4)	1158(4)	9980(1)	11(1)	2072(4)	1155(4)	9975(2)	18(1)
O16	−1568(4)	−520(4)	7672(2)	10(1)	−1583(4)	−502(3)	7678(1)	15(1)
O17	5248(4)	−371(4)	8950(2)	10(1)	5249(3)	−366(4)	8947(2)	19(1)
O18	−870(4)	6135(4)	8752(1)	9(1)	−876(3)	6140(3)	8758(1)	13(1)
O19	−1615(4)	2062(4)	8904(2)	14(1)	−1612(4)	2064(4)	8911(2)	21(1)
O20	−4331(4)	−2976(4)	6676(2)	16(1)	−4330(4)	−2949(5)	6686(2)	26(1)

U_{eq} is defined as one third of the trace of the orthogonalized U_{ij} tensor.
[a]Anisotropic displacement parameters for Na at 293 and 105 K

(K)	U_{11} (Å^2)	U_{22} (Å^2)	U_{33} (Å^2)	U_{23} (Å^2)	U_{13} (Å^2)	U_{12} (Å^2)
293	0.0227(9)	0.0202(9)	0.200(4)	−0.0037(14)	−0.0387(15)	−0.0027(7)
105	0.0145(8)	0.0124(7)	0.111(2)	−0.0014(10)	−0.0221(11)	−0.0017(6)

3. Results and discussion

3.1. Crystal structure

The crystal structure analysis of $NaMg_3Al(MoO_4)_5$ confirms that the compound crystallizes in the structure known earlier for $NaMg_3In(MoO_4)_5$ [15] and $NaFe_4(MoO_4)_5$ [9]. The final atomic coordinates and equivalent thermal displacement parameters are given in Table 2. Note that full temperature displacement tensor is given only for sodium atom. Relevant interatomic distances are listed in Table 3. Supplementary data are available from the Fachinformationszentrum (FIZ) Karlsruhe, Informationsdienst ICSD, D-76344 Eggenstein-Leopoldshafen, Germany (e-mail: crysdata@fiz-karlsruhe.de) under the CSD no. 391347 (for the structure at 105 K) and 391348 (for the structure at 293 K).

The structure is composed of a three-dimensional network of $[MgO_6]$ and $[AlO_6]$ octahedra and $[MoO_4]$ tetrahedra (Fig. 1). While Mo tetrahedra are separated from each other sharing corners with other polyhedra, the Mg and Al octahedra are linked to each other by edge-sharing forming trimers. Sodium atoms are located in the cavities with five-fold Na–O coordination.

The comparison of the structure parameters obtained at two different temperatures (cf. Table 1) shows rather slight differences: positional parameters remain almost the same, temperature displacement parameters decrease by factor of 2 when temperature goes down from RT to 105 K. Fig. 2 shows sodium coordination polyhedron determined at RT (a) and at 105 K (b). The polyhedron has a shape of distorted pyramid with the Na atom located uncentrically inside it. The most intense thermal vibrations of sodium occur more or less along *c*-direction, almost perpendicularly to the plane defined by O6, O11 and O12 atoms, towards the O4–O11–O20 plane. It is seen that the general shape and most bond lengths do not change distinctly with temperature. The only distinct influence of temperature is the shift of sodium towards the center of the pyramid which manifests itself in the decreasing of the bond length to O4.

Our investigations confirmed that the thermal behavior of sodium is hardly described by the formalism of anisotropic temperature factors. Table 1 contains information on the largest differential peaks and holes in the electron density calculated. It appears that all largest peaks for both temperatures are located in the vicinity of sodium atoms. It means that the ellipsoid approximating thermal behavior of sodium is not adequate and should be replaced by more complex construction. Two interpretations can be taken into account: another, more complex approximation of the thermal motion (e.g. anharmonic one), or certain kind of disorder, causing the splitting of the sodium position into several ones. It is not easy to settle this problem using conventional X-ray structure analysis. We tried only to check to what extent the better approximation of thermal behavior of sodium can improve the quality of structure refinement. For this purpose we performed the structure refinements for the sodium atom with isotropic displacement factors fixed at the values typical for certain temperatures (0.015 and 0.010 $Å^2$, for 293 and 105 K, respectively) and split in order to eliminate all differential peaks near the sodium position. It appears that for both temperatures studied it is necessary to split its position into

Table 3
Bond lengths for Mo–O tetrahedra, Mg–O and Al–O octahedra and Na–O polyhedron in $NaMg_3Al(MoO_4)_5$ at 105 and at 293 K

Atom1	Atom2	Bond length (Å) at 105 K	Bond length (Å) at 293 K
Mo1	O15	1.729(3)	1.725(3)
Mo1	O17	1.739(3)	1.732(2)
Mo1	O1	1.787(2)	1.792(2)
Mo1	O14	1.814(3)	1.816(2)
Mo2	O5	1.730(3)	1.731(3)
Mo2	O10	1.754(3)	1.749(2)
Mo2	O16	1.776(2)	1.771(2)
Mo2	O11	1.791(2)	1.797(2)
Mo3	O2	1.745(3)	1.738(2)
Mo3	O9	1.756(3)	1.751(2)
Mo3	O3	1.757(2)	1.753(3)
Mo3	O8	1.802(2)	1.805(2)
Mo4	O7	1.739(3)	1.738(3)
Mo4	O6	1.750(3)	1.745(3)
Mo4	O19	1.762(3)	1.755(2)
Mo4	O18	1.801(2)	1.804(2)
Mo5	O20	1.719(3)	1.713(3)
Mo5	O4	1.756(3)	1.750(3)
Mo5	O13	1.772(3)	1.766(3)
Mo5	O12	1.831(3)	1.836(2)
Mg1	O5	2.000(3)	1.997(3)
Mg1	O2	2.010(2)	2.007(3)
Mg1	O4	2.047(3)	2.052(3)
Mg1	O9	2.047(3)	2.051(3)
Mg1	O8	2.074(3)	2.079(2)
Mg1	O8	2.078(3)	2.082(3)
Mg2	O1	2.023(3)	2.020(2)
Mg2	O6	2.024(3)	2.020(2)
Mg2	O7	2.023(3)	2.024(3)
Mg2	O14	2.033(3)	2.033(2)
Mg2	O18	2.081(3)	2.086(2)
Mg2	O12	2.097(3)	2.103(3)
Mg3	O19	2.021(3)	2.023(3)
Mg3	O16	2.065(3)	2.066(3)
Mg3	O17	2.077(3)	2.073(3)
Mg3	O18	2.079(3)	2.075(2)
Mg3	O15	2.080(3)	2.086(3)
Mg3	O1	2.106(3)	2.109(2)
Al	O3	1.946(3)	1.946(3)
Al	O10	1.973(3)	1.967(3)
Al	O14	1.976(3)	1.980(3)
Al	O13	1.982(3)	1.981(3)
Al	O11	2.015(3)	2.019(3)
Al	O12	2.054(3)	2.055(3)
Na	O20	2.235(3)	2.217(3)
Na	O11	2.331(3)	2.324(3)
Na	O16	2.393(3)	2.403(4)
Na	O12	2.565(3)	2.565(3)
Na	O4	2.694(4)	2.733(4)

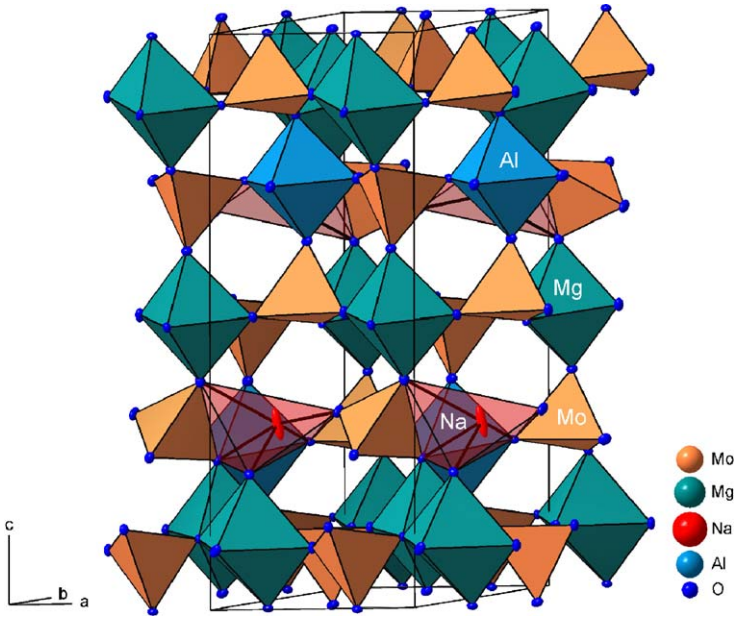

Fig. 1. Crystal structure of $NaMg_3Al(MoO_4)_5$.

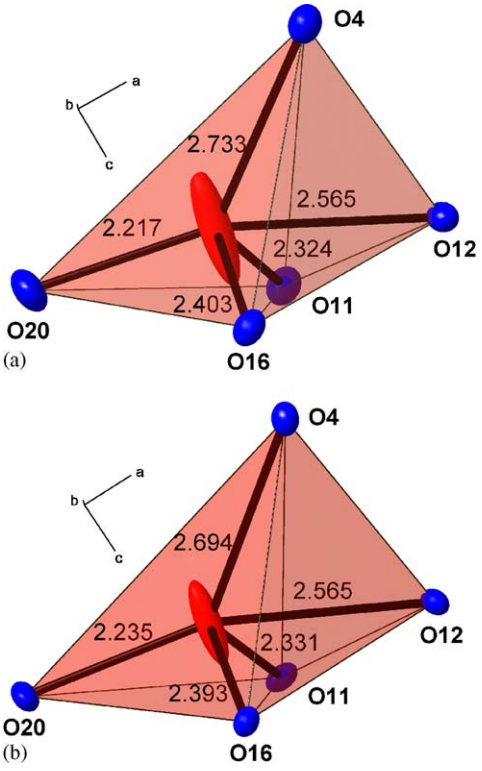

Fig. 2. Coordination polyhedra of Na at 293 K (a) and 105 K (b). Bond lengths (Å) are shown. Atoms are represented by their thermal displacement ellipsoids.

four contributors occupied in a different manner. Table 4 contains numerical results and Fig. 3 shows the positions of all four Na contributors in the cavity formed by Mo tetrahedra and Mg octahedra. For both temperatures the Na contributors are spread out over the same distance of 1.37 Å forming a shape of crescent. The distances between contributors do not change with temperature, while changes are observed for their occupation parameters. The refinement performed in the presented way eliminated completely differential peaks near Na atoms and decreased general values of residues to 0.75 and $-0.83\,e/Å^3$ for 293 K and to 1.34 and $-1.17\,e/Å^3$ for 105 K (cf. data in Table 1 for unsplit Na). For both temperatures the strongest differential peaks were located near Mo atoms. Flattening of the differential electron density resulted in decreasing of R indices. Final R_1 decreased from 0.026 to 0.023 for 293 K, and from 0.029 to 0.027 for 105 K.

3.2. Selection rules and vibrational modes

The factor group analysis predicts that there should be $90A_g+90A_u$ ($\mathbf{k}=0$) unit cell modes for the triclinic $P\bar{1}$ structure (cf. Table 5). Since Mo–O bonds are much stronger than the Al–O, Mg–O and Na–O bonds, the structure can be considered as built of MoO_4^{2-}, Al^{3+}, Mg^{2+} and Na^+ ions. The vibrational modes can be, therefore, subdivided into $20A_g+20A_u$ stretching modes of the MoO_4^{2-} tetrahedra, $25A_g+25A_u$ bending modes of the MoO_4^{2-} tetrahedra, $15A_g+15A_u$ translational motions of the MoO_4^{2-} ions, $15A_g+15A_u$ librational motions of the MoO_4^{2-} ions, $3A_g+3A_u$ translational motions of the Na^+ ions, $9A_g+9A_u$ translational motions of the Mg^{2+} ions and $3A_g+3A_u$ translational motions of the Al^{3+} ions. It should be noticed, however, that from the $15A_g+15A_u$ translational motions the $3A_u$ acoustic modes should be subtracted. The A_g modes are Raman-active and A_u modes IR-active.

The recorded IR and Raman spectra are presented in Figs. 4 and 5, and the measured wavenumbers are listed in

Table 4
Atomic parameters of Na as results of the structure refinement with sodium split into 4 contributors with fixed isotropic thermal displacement and occupation parameter refined

Atom	105 K					293 K				
	x	y	z	U_{iso} (Å^2)	Occupation[a]	x	y	z	U_{iso} (Å^2)	Occupation[a]
Na1	0.1008	0.3381	0.3281	0.010	0.280	0.0986	0.3451	0.3374	0.015	0.182
Na2	0.1099	0.3325	0.3080	0.010	0.499	0.1067	0.3296	0.3158	0.015	0.405
Na3	0.1323	0.3408	0.2776	0.010	0.178	0.1241	0.3357	0.2905	0.015	0.246
Na4	0.1257	0.3515	0.2502	0.010	0.057	0.1360	0.3459	0.2609	0.015	0.139

[a]Occupation was not constrained to give 1 as a sum of four contributors.

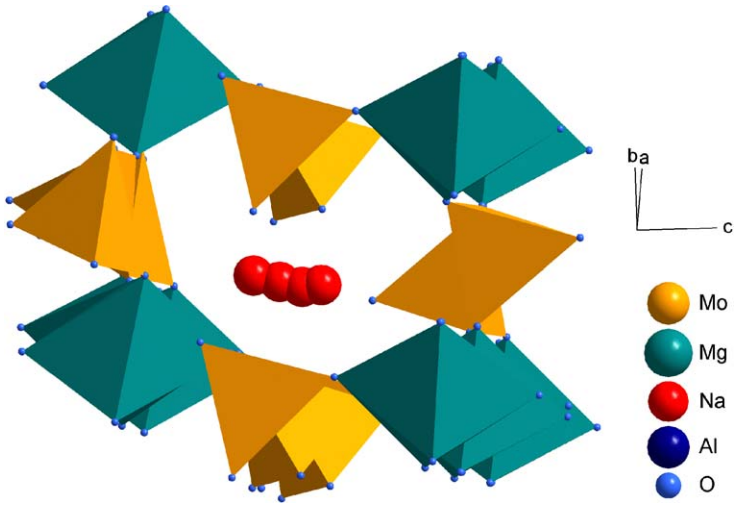

Fig. 3. The splitting of sodium position into four contributors in the cavity formed by Mo tetrahedra and Mg octahedra. Al octahedra closing the cavity are not shown for the clarity. The figure shows the result obtained for 293 K. Results for 105 K are very similar.

Table 5
Factor group analysis for $P\bar{1}$ structure of $NaMg_3Al(MoO_4)_5$

C_i symmetry	$n(N)$	$n(i)$	$n(L)$	$n(T'(MoO_4))$	$n(T'(Na^+))$	$n(T'(Al^{3+}))$	$n(T'(Mg^{2+}))$	$n(T)$	IR	RS
A_g	90	45	15	15	3	3	9	0	—	xx, yy, zz xy, yz, xz
A_u	90	45	15	15	3	3	9	3	x, y, z	—

$n(N)$ overall degrees of freedom, $n(i)$—internal vibrations, $n(L)$—libratory lattice modes, $n(T')$—translatory lattice modes, $n(T)$—acoustic modes.

Table 6. A total number of 24 Raman and 31 IR modes could be identified. This number is much smaller than predicted by group theory because the five crystallographically non-equivalent MoO_4^{2-} tetrahedra have similar Mo–O bond lengths and, therefore, many phonons have very similar energy and are not resolved in our experiment. Based on vibrational studies of a number of molybdates [20,26–28], we may unambiguously assign the 660–1010 cm^{-1} bands to stretching modes of the MoO_4^{2-} tetrahedra. It is worth noting that some stretching modes are observed at relatively low energy, i.e. in the 660–750 cm^{-1} region (cf. Table 6). Such low energy of some modes is not typical for tetrahedral coordination of Mo atoms. Significant shift of some stretching vibrations towards lower wavenumbers is, however, observed when a significant dipole–dipole interactions between MoO_4^{2-} ions occurs [29–31]. It can be concluded, therefore, that the observation of the modes in the 660–750 cm^{-1} region indicates presence of significant interactions between the MoO_4^{2-} ions in the $NaMg_3Al(MoO_4)_5$ structure.

Bending and lattice vibrations are observed below 500 cm^{-1}. The detailed assignment of the observed modes would be possible by comparison of the spectral data for a few isostructural $NaM_3^{II}M^{III}(MoO_4)_5$ molybdates. Unfortunately, no IR and Raman data are available for any member of this family of molybdates. Some data have, however, been published for $KMgSc(MoO_4)_3$ and $KMgLu(MoO_4)_3$ molybdates which crystallize in a similar

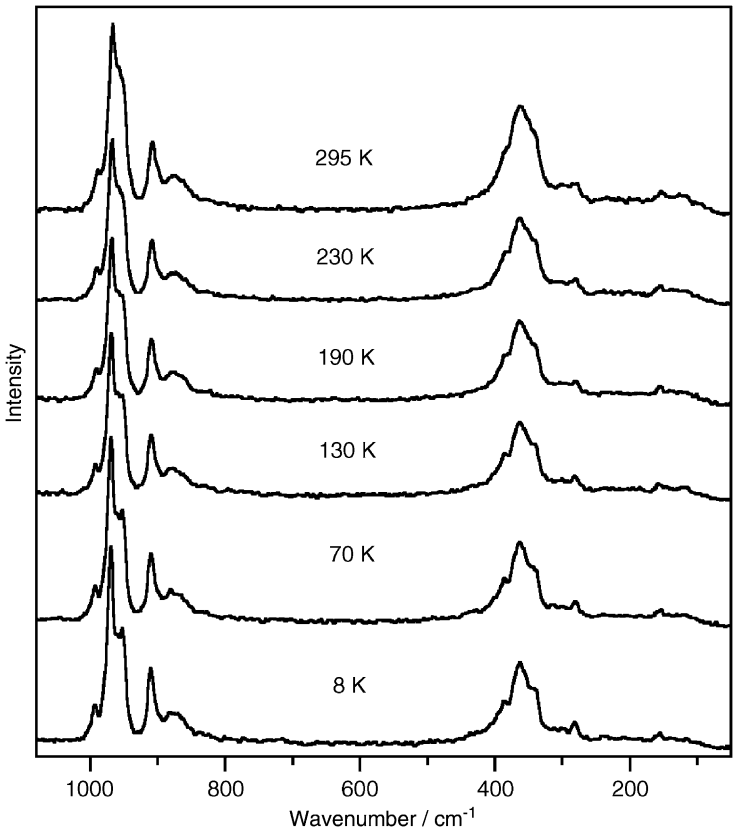

Fig. 4. Temperature-dependent Raman spectra of $NaMg_3Al(MoO_4)_5$.

type of structure as $NaMg_3Al(MoO_4)_5$ [32]. These data show that bending modes are observed at 300–410 cm^{-1} [32]. In case of $NaMg_3Al(MoO_4)_5$ bending vibrations of the MoO_4^{2-} ions contribute to the bands observed in the 320–500 cm^{-1} region. Due to smaller atomic mass of Al in comparison with Sc, translations of the Al^{3+} ions are expected to be observed at significantly higher wavenumbers than translations of Sc^{3+} ions, which were located near 190 cm^{-1} for $KMgSc(MoO_4)_3$ [32]. Our previous studies and lattice dynamics calculations, performed for a few aluminum containing molybdates, showed that translational motions of the Al^{3+} ions may significantly contribute to vibrations observed in the 320–500 cm^{-1} region [26–28]. This result shows that the bands in the 320–500 cm^{-1} region should be assigned to the bending modes coupled to the translations of the Al^{3+} ions. Based on previous lattice dynamics calculations of layered molybdates [27,28] and studies of $KMgSc(MoO_4)_3$ and $KMgLu(MoO_4)_3$ molybdates [32], we may assign the modes in the 250–320 cm^{-1} region to translations of the MoO_4^{2-} and Na^+ ions with smaller contribution of the $T'(Al^{3+})$ motions. The modes below 250 cm^{-1} can be assigned to coupled librations and translations of the MoO_4^{2-} ions. As far as the $T'(Mg^{2+})$ modes are concerned, they are expected to be observed at smaller wavenumbers that the $T'(Al^{3+})$ modes because the strength of metal–oxygen bond is larger for the trivalent aluminum than for divalent magnesium. The former studies of $MgAl_2O_4$ spinel showed that translations of Mg^{2+} ions are located below 250 cm^{-1} [33]. On the other hand, studies of $KMgSc(MoO_4)_3$ and $KMgLu(MoO_4)_3$ molybdates suggested that magnesium ions contribute significantly to a few vibrations in the 90–280 cm^{-1} region [32]. In case of $NaMg_3Al(MoO_4)_5$ these modes are most likely located in the 150–250 cm^{-1} region.

The temperature-dependent studies show no changes which could indicate that this molybdate exhibits a phase transition. We only observe the typical decrease of bandwidths with decreasing temperature, leading to better resolution of bands at low temperatures. However, this decrease is small and the bandwidth of many modes exceeds 15 cm^{-1} even at 8 K. This result indicates that many of the observed bands are composed of a few bands of very similar energy, not resolved even at the lowest temperature. It also points to weak anharmonicity of the phonons. The observed wavenumber changes in the 8–295 K temperature range are also weak, a few cm^{-1} for majority of modes. This result indicates weak changes in the bond lengths with temperature.

3.3. Electron absorption and luminescence spectra

The RT absorption and excitation spectra of the Cr^{3+} doped in $NaMg_3Al(MoO_4)_5$ crystals are presented in Fig. 6. The absorption spectrum of Cr^{3+} ions consists mainly of two peaks at approximately 479 and 694 nm.

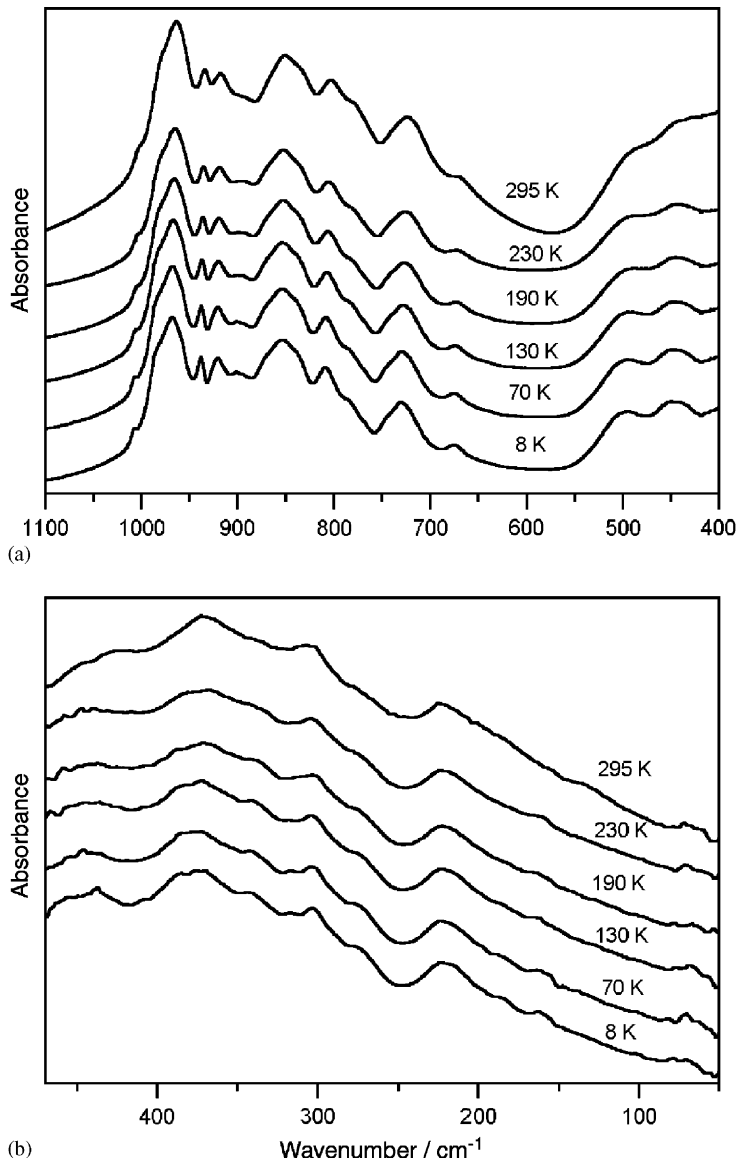

Fig. 5. Temperature-dependent IR spectra of $NaMg_3Al(MoO_4)_5$ in the high-frequency (a) and low-frequency (b) region.

These bands are due to the absorption transition from $^4A_2$ ground state of Cr^{3+} ions to the $^4T_2$ and $^4T_1$ excited states, respectively, and are attributed to the presence of Cr^{3+} ion in six-coordinated environment [34]. The band of the $^4A_2 \rightarrow {}^4T_2$ transition has a noticeable splitting which arises due to Fano-type antiresonance [35] as a result of an interaction between the sharp intraconfigurational t_2^3e (^2E and $^2T_1$) and vibronically broadened $^4T_2$ (t_2^3e) levels. On the basis of our earlier studies on optical properties of other molybdate hosts doped by Cr^{3+} ions [36–38] the characteristic dips observed at 727 and 693 nm in this band shape can be assigned to $^4A_2 \rightarrow {}^2E$ and $^4A_2 \rightarrow {}^2T_1$ absorption, respectively. The $^4A_2 \rightarrow {}^4T_1$(P) transition is responsible for a strong edge observed below 400 nm. The low-temperature absorption measurements down to 10 K show no noticeable changes in the observed spectral contour.

In order to discuss the optical behavior of the active center the crystal field strength Dq and the Racah parameters B and C should be derived from the experimental data. For the octahedral symmetry approximation the energy of the $^4A_2 \rightarrow {}^4T_2$ absorption band gives directly the value of 10Dq which is equal to 14,400 cm^{-1}. The value of B parameter, determined from the energy separation Δ between the $^4A_2 \rightarrow {}^4T_2$ and $^4A_2 \rightarrow {}^4T_1$ absorption peaks, was evaluated from the expression [39],

$$B/\mathrm{Dq} = [(\Delta/\mathrm{Dq})^2 - 10(\Delta/\mathrm{Dq})]/15(\Delta/\mathrm{Dq} - 8), \quad (1)$$

where Δ is the energy difference between the $^4A_2 \rightarrow {}^4T_2$ and $^4A_2 \rightarrow {}^4T_1$ absorption bands. The value of B was found to be 676 cm^{-1}. The C parameter is calculated from the position of the $^4A_2 \rightarrow {}^2E$ absorption peak using the equation [39]:

$$E(^2E)/B = 3.05(C/B) + 7.9 - 1.8(B/\mathrm{Dq}). \quad (2)$$

The calculated value for $NaMg_3Al(MoO_4)_5$ is 2945 cm^{-1}.

Table 6
Raman and IR wavenumbers (in cm^{-1}) observed at 295 and 8 K temperature together with the proposed assignment

Raman		IR		Assignment
295 K	8 K	295 K	8 K	
989.3w	994.3w	1003.5sh	1008.1vw	
—	979.4sh	980.9sh	986.2sh	
967.0s	967.0s	962.3s	970.9s	v_1
956.4w	959.2w	—	962.1sh	
949.5w	951.6m	934.9m	938.6m	
908.3m	910.8m	914.8m	921.9m	
900.1sh	903.3sh	898.9w	901.6w	
879.2m	882.9m	889.3w	892.1w	
863.6sh	868.5m	869.0sh	872.2sh	
—	—	852.8s	853.0s	
824.8w	830.9vw	832.5sh	835.7sh	v_3
793.3vw	—	802.7s	808.1s	
766.9vw	—	776.3sh	783.7sh	
—	—	741.0sh	746.8sh	
—	—	722.4m	726.8m	
—	—	665.9w	672.8w	
—	—	498.4m	502.9m	
427.1vw	429.1vw	443.4m	454.3m	
—	397.3sh	424.9m	437.3m	v_2 and v_4 modes coupled to $T'(Al^{3+})$
388.4sh	387.5w	380.9sh	385.6s	
362.5s	362.7s	368.8s	373.3s	
341.9sh	340.6w	336.7m	336.5m	$T'(MoO_4)$, $T'(Na^+)$ and $T'(Al^{3+})$
—	—	—	318.1w	
301.1w	300.0w	303.4m	302.1m	
280.6w	281.9w	273.2sh	273.1w	
236.7vw	238.9vw	224.7m	222.8m	$L(MoO_4)$ coupled to $T'(MoO_4)$ and $T'(Mg^{2+})$
209.0vw	208.6vw	—	—	
189.6vw	187.3vw	—	185.2w	
154.9w	157.3w	—	160.9w	
135.6vw	135.9vw	—	—	
115.9vw	116.0vw	—	—	
—	100.2vw	72.0vw	79.1vw	$L(MoO_4)$ coupled to $T'(MoO_4)$
		67.5vw	71.1vw	
		60.2vw	67.1vw	

v_1, v_3, v_2 and v_4 denote symmetric stretching, asymmetric stretching, symmetric bending and asymmetric bending vibrations of MoO_4^{2-} unit, respectively. $T'(Al^{3+})$, $T'(MoO_4)$, $T'(Mg^{2+})$ and $L(MoO_4)$ denote translations of Al^{3+}, MoO_4^{2-} and Mg^{2+} ions, and librations of MoO_4^{2-} ions, respectively.

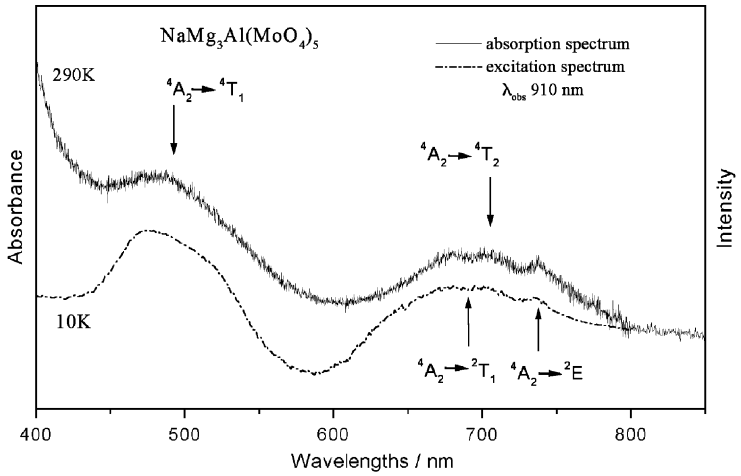

Fig. 6. Room temperature absorption and excitation spectra of $NaMg_3Al(MoO_4)_5:Cr^{3+}$.

The energy values of the Cr^{3+} ion levels calculated from the absorption spectrum are shown in Table 7, together with the crystal field and Racah parameters. The value of the Dq/B ratio, equal to 2.13, shows that the field is rather weak and indicates that the Cr^{3+} ions are in low ligand field with the minimum of the $^4T_2$ level lying below the minimum of the ^2E state. From this point of view we should observe broadband emission.

Fig. 7 shows the emission of Cr^{3+} ion in $NaMg_3Al(MoO_4)_5$ at several temperatures: RT, 200, 100 and 10 K upon excitation at 491 nm. The observed spectra are dominated by broadband emission at 904 nm which is attributed to $^4T_2 \rightarrow {}^4A_2$ emission of Cr^{3+} ions located at sites with low strength of crystalline field. With lowering temperature down to 10 K the emission intensity strongly increases without any noticeable changes in peak energy. It can be noticed that apart from the broadband emission, a few week and sharp lines appear at high-energy side of registered spectra. It is well known that Cr^{3+} ion in ruby [40] gives the R lines when Cr^{3+} is substituted in an α-Al_2O_3 structure and the ion is surrounded by a distorted octahedron of nearest-neighbor O^{2-} ions. The Cr^{3+} ions are at sites of trigonal symmetry, so crystalline field energy splits the ^2E state into R_1 and R_2 component at 693.0 and 694.4 nm, respectively. Therefore, the weak sharp lines observed by us lying at about 693 nm and their similarity to ruby lines indicate that the $^2E \rightarrow {}^4A_2$ emission occurs in the studied crystal. The observation of this emission points out to presence of additional luminescent sites with the Cr^{3+} ions in high ligand field with the minimum of the $^4T_2$ level lying above the minimum of the ^2E state. The observation of different luminescent sites is consistent with the results of the X-ray analysis, since in the $NaMg_3Al(MoO_4)_5$ host the Cr^{3+} ions may substitute for both Mg^{2+} and Al^{3+} ions. The inspection of Table 3 shows that there are three available Mg^{2+} sites with Mg–O distances ranging from 1.997 to 2.110 Å and one Al^{3+} site with Al–O distances ranging from 1.945 to 2.054 Å. Because the Al–O distances are shorter than the Mg–O ones, it seems that the crystal field strength should be larger for those Cr^{3+} ions which substitute for Al^{3+} ions. However, this view is over-simplified since the substitution of Cr^{3+} ions for Mg^{2+} and Al^{3+} ions should change the active ion—oxygen distances due to difference in ionic radii of these ions. The substitution of smaller aluminum ions (ionic radius 0.53 Å) by larger chromium ions (ionic radius 0.615 Å) should lead to increase of the site size and subsequently to decrease of the crystal field strength of the Cr^{3+} ion. On contrary, the substitution of larger Mg^{2+} ions (ionic radius 0.72 Å) by smaller Cr^{3+} ions should lead to an increase of the crystal field strength for these sites. Moreover, when Mg^{2+} ions are substituted by Cr^{3+} ions, a charge compensation is required, which can result in e.g. a nearest cation vacancy. Such compensation will result in the local symmetry deformation of the octahedrally coordinated Cr^{3+} ion site and changes in the crystal field strength [41–43]. The above discussion shows that the crystal field

Table 7
Room temperature energy of the electron transitions and crystal field parameters of the Cr^{3+} ions located at sites with low strength of crystalline field

$^4A_2 \rightarrow {}^2E$ (cm^{-1})	~13755
$^4A_2 \rightarrow {}^4T_2$ (cm^{-1})	14440
$^4T_2 \rightarrow {}^4A_2$ (cm^{-1})	11065
$^4A_2 \rightarrow {}^2T_1$ (cm^{-1})	14434
$^4A_2 \rightarrow {}^4T_1(F)$ (cm^{-1})	20860
$^4A_2 \rightarrow {}^4T_1(P)$ (cm^{-1})	>28650
Dq (cm^{-1})	1440
B (cm^{-1})	676
Dq/B	2.13
C (cm^{-1})	2945
C/B	4.36

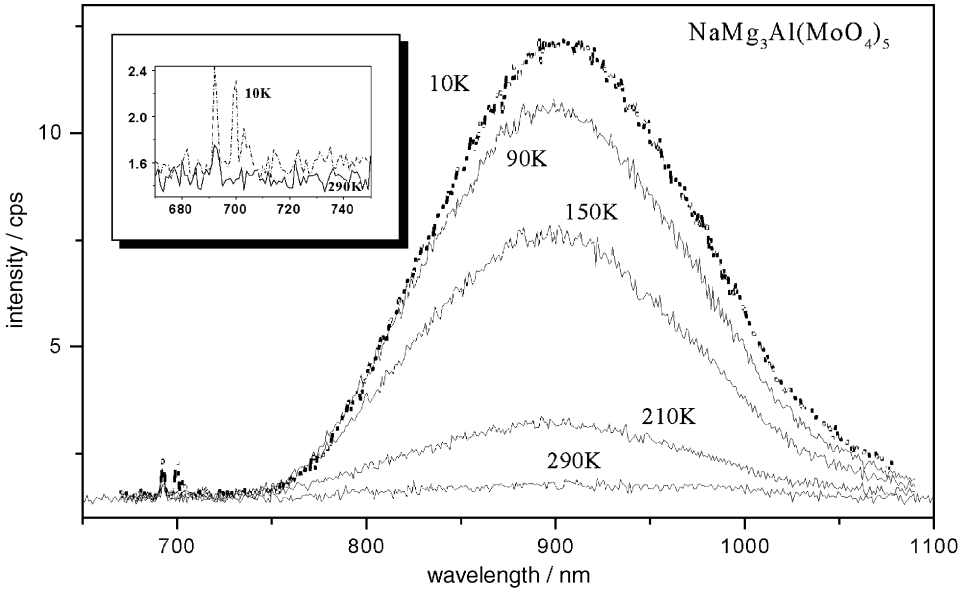

Fig. 7. Emission spectra of $NaMg_3Al(MoO_4)_5$:Cr^{3+} at several temperatures upon 491 nm excitation.

strength of chromium in the studied crystal depends on many factors and therefore the assignment of chromium sites is not possible on the basis of present experimental results. Detailed discussion on luminescence properties of Cr^{3+} ion and characteristics of existing sites requires additional optical measurements and will be a subject of our future study.

4. Conclusions

The X-ray, IR, Raman, electron absorption, excitation and luminescence studies have been performed for $NaMg_3Al(MoO_4)_5$ crystals doped with Cr^{3+} ions. The studies show that this compound crystallizes in the same structure as $NaMg_3In(MoO_4)_5$. However, In^{3+} and Mg^{2+} ions are statistically distributed among the same sites, whereas Al^{3+} and Mg^{2+} ions are ordered. Our results indicate that Cr^{3+} ions substitute for both Al^{3+} and Mg^{2+} giving rise to both narrow $^2E \rightarrow {}^4A_2$ emission, typical for chromium in high ligand field, and $^4T_2 \rightarrow {}^4A_2$ emission, characteristic for chromium in low ligand field.

The X-ray analysis shows also that thermal displacement parameter for sodium is enormously large and strongly anisotropic, even at low temperature of 105 K, and cannot be described by the formalism of anisotropic temperature factors. Two interpretations can be taken into account: more complex approximation of the thermal motion or certain kind of disorder, causing the splitting of the sodium position into several ones. Our results do not allow us to obtain precise and definitive conclusions about the nature of this phenomenon. However, we were capable of obtaining the rough approximation of sodium motion by determining crescent-like spreading of his electron density.

The temperature-dependent X-ray diffraction studies show that this material does not exhibit any phase transition and that bond lengths do not change distinctly with temperature. As a result, the observed temperature changes in vibrational and electronic properties are weak.

Acknowledgment

We would like to thank Professor A. Pietraszko for his help in X-ray measurements.

References

[1] H. Kato, N. Matsudo, A. Kudo, Chem. Lett. 33 (2004) 1216.
[2] A. Maione, M. Devillers, J. Solid State Chem. 177 (2004) 2339.
[3] H. Canibano, G. Boulon, L. Palatella, Y. Guyot, A. Brenier, M. Voda, R. Balda, J. Fernandez, J. Lumin. 102 (2003) 318.
[4] A. Mendez-Blas, M. Rico, V. Volkov, C. Cascales, C. Zaldo, C. Coya, A. Kling, L.C. Alves, J. Phys.: Condens. Matter. 16 (2004) 2139.
[5] F. Goutenoire, O. Isnard, E. Suard, O. Bohnke, Y. Laligant, R. Retoux, P. Lacorre, J. Mater. Chem. 11 (2001) 119.
[6] I.Y. Kotova, N.M. Kozhevnikova, Inorg. Mater. 34 (1998) 1068.
[7] N.M. Kozhevnikova, I.Y. Kotova, Inorg. Mater. 34 (1998) 1071.
[8] I.Y. Kotova, N.M. Kozhevnikova, Russ. J. Appl. Chem. 76 (2003) 1572.
[9] E. Muessig, K.G. Bramnik, H. Ehrenberg, Acta Crystallogr. B 59 (2003) 611.
[10] K. Ivanov, S. Krustev, P. Litcheva, J. Alloys Compd. 279 (1998) 132.
[11] Y.J. Zhang, I. Rodriguez-Ramos, A. Guerrero-Ruiz, Catal. Today 61 (2000) 377.
[12] M.M. Barsan, F.C. Thyrion, Catal. Today 81 (2003) 159.
[13] A.P.V. Soares, M.F. Portela, Catal. Rev. 47 (2005) 125.
[14] N.M. Kozhevnikova, M.V. Mokhosoev, F.P. Alekseev, Z.I. Khazheeva, Ye.R. Abykova, S.D. Tudupova, Zh. Neorg. Khim. 34 (1989) 1837.
[15] R.F. Klevtsova, A.D. Vasilev, N.M. Kozhevnikova, L.A. Glinskaya, A.I. Kruglik, I.Y. Kotova, Zh. Strukt. Khim. 34 (1993) 147.
[16] A.W. Sleight, L.H. Brixner, J. Solid State Chem. 7 (1973) 172.
[17] A.K. Tyagi, S.N. Achary, M.D. Mathews, J. Alloys Compd. 339 (2002) 207.
[18] J.S.O. Evans, T.A. Mary, A.W. Sleight, J. Solid State Chem. 137 (1998) 148.
[19] R.A. Secco, H. Liu, N. Imanaka, G. Adachi, M.D. Rutter, J. Phys. Chem. Solids 63 (2002) 425.
[20] W. Paraguassu, M. Mączka, A.G. Souza Filho, P.T.C. Freire, J. Mendes Filho, F.E.A. Melo, L. Macalik, L. Gerward, J. Staun Olsen, A. Waśkowska, J. Hanuza, Phys. Rev. B 69 (2004) 94111.
[21] R.F. Klevtsova, P.V. Klevtsov, Kristallografiya 17 (1972) 955.
[22] R.F. Klevtsova, L.P. Kozeeva, P.V. Klevtsov, Kristallografiya 20 (1975) 925.
[23] R.F. Klevtsova, L.A. Gaponenko, L.A. Glinskaya, E.S. Zolotova, N.V. Podberezskaya, P.V. Klevtsov, Kristallografiya 24 (1979) 751.
[24] R.F. Klevtsova, V.G. Kim, P.N. Klevtsov, Kristallografiya 25 (1980) 1148.
[25] G.M. Sheldrick, SHELX-97, University of Göttingen, Germany, 1997.
[26] M. Mączka, W. Paraguassu, A.G. Souza Filho, P.T.C. Freire, J. Mendes Filho, F.E.A. Melo, J. Hanuza, J. Solid State Chem. 177 (2004) 2002.
[27] W. Paraguassu, A.G. Souza Filho, M. Mączka, P.T.C. Freire, F.E.A. Melo, J. Mendes Filho, J. Hanuza, J. Phys.: Condens. Matter 16 (2004) 5151.
[28] M. Mączka, K. Hermanowicz, P.E. Tomaszewski, J. Hanuza, J. Phys.: Condens. Matter 16 (2004) 3319.
[29] J.F. Scott, J. Chem. Phys. 49 (1968) 98.
[30] A. Jayaraman, B. Batlogg, L.G. VanUitert, Phys. Rev. B 28 (1983) 4774.
[31] J.S.O. Evans, Z. Hu, J.D. Jorgensen, D.N. Argyriou, S. Short, A.W. Sleight, Science 275 (1997) 61.
[32] M.V. Mokhosoev, I.I. Murzakhanova, N.M. Kozhevnikova, V.V. Fomichev, Zh. Neorg. Khim. 36 (1991) 1273.
[33] H. Kojitani, K. Nishimura, A. Kubo, M. Sakashita, K. Aoki, M. Akaogi, Phys. Chem. Miner. 30 (2003) 409.
[34] A.B.P. Lever, Inorganic Electronic Spectroscopy, Elsevier Publishing Company, Amsterdam, London, New York, 1968.
[35] A. Lempicki, L. Andrews, S.J. Nettel, B.C. McCollum, E.I. Solomon, Phys. Rev. Lett. 44 (1980) 1234.
[36] K. Hermanowicz, M. Mączka, P.J. Dereń, J. Hanuza, W. Stręk, H. Drulis, J. Lumin. 92 (2001) 151.
[37] K. Hermanowicz, J. Lumin. 109 (2004) 9.
[38] K. Hermanowicz, J. Hanuza, M. Mączka, P.J. Dereń, E. Mugeński, H. Drulis, I. Sokólska, J. Sokolnicki, J. Phys.: Condens. Matter. 13 (2001) 5807.
[39] B. Henderson, G.F. Imbush, Optical Spectroscopy of Inorganic Solids, Clarendon Press, Oxford, 1989.
[40] J.H. Eggert, K.A. Goettel, I.F. Silvera, Phys. Rev. B 40 (1989) 5724.
[41] P.J. Dereń, M. Malinowski, W. Strek, J.Lumin. 68 (1996) 91.
[42] M. Grinberg, K. Holliday, J.Lumin. 92 (2001) 277.
[43] B. Henderson, M. Yamaga, Y. Gao, K.P. O'Donnell, Phys. Rev.B 46 (1992) 652.